

## A SILVER-NANOPARTICLE-EMBEDDED ACTIVATED-CARBON-PEDOT:PSS COMPOSITE CONDUCTOR FOR ENHANCING ELECTRICAL CONDUCTIVITY OF A GAS SENSOR MODULE

M. LEE<sup>a†</sup>, Y. JANG<sup>a†</sup>, J. OH<sup>b†</sup>, J. JUNG<sup>b,\*</sup>

<sup>a</sup>*Department of Mechanical Design Engineering, College of Engineering, Chonbuk National University, Jeonju 54896, South Korea*

<sup>b</sup>*Department of Nano-bio Mechanical System Engineering, College of Engineering, Chonbuk National University, Jeonju 54896, South Korea*

This study focused on the development of a gas sensor module based on a highly sensitive activated-carbon-PEDOT:PSS three-dimensional (3D) conductive composite. The activated-carbon-PEDOT:PSS conductive composite was quantified by forming it into a 3D structure. The best activated carbon among four types was selected in terms of the specific surface area, pore volume, mean pore diameter, and ash content analysis. The conductive composite was fabricated by combining pulverized activated carbon and PEDOT:PSS. The electrical conductivity of the composite was enhanced by doping with ethylene glycol and silver nanoparticles. A gas sensor module base was fabricated in the mold, and a pair of gold electrodes was fabricated on the gas sensor module using an e-beam evaporator. The activated-carbon-PEDOT:PSS composite-based gas sensor module was evaluated to investigate the gas adsorption performance and conductivity. In the ethanol gas adsorption experiment, the highly sensitive change in the resistance of the conductive composite was confirmed. The results of the study can be useful for a variety of bio-applications.

(Received February 2, 2018; Accepted June 2, 2018)

*Keywords:* Activated carbon, PEDOT:PSS, Composite conductor, Gas adsorption, Gas sensor module

### 1. Introduction

In the crystal structure of activated carbon, net planes are similar to graphite crystal structures because they are parallel and have constant intervals; layer planes are spaced at different intervals, and the layers are irregularly stacked, resulting in an incomplete shape. Such an array is called a turbostratic structure, or amorphous structure [1]. Activated carbon has pore structures, such as micropores, mesopores, and macropores, as its basic crystals are irregularly arranged [2]. This plays a very important role in adsorbing gas molecules.

The size of the micropores in activated carbon can be controlled from several micrometers to several nanometers, and activated carbon has a high specific surface area of over 1000 m<sup>2</sup>/g [3,4]. In addition, its application to sensors is possible because it can adsorb gases, even at room temperature, and has excellent electrical conductivity. It is also much more competitive in price than other adsorbent materials [5].

Kim et al. (2006) investigated the adsorption capacity and desorption characteristics of impregnated activated carbon (IAC) prepared with various acids and bases for application to the adsorption part of adsorption-desorption in a catalytic oxidation hybrid system [6]. Sumathi et al. (2009) examined the individual and simultaneous adsorption of SO<sub>x</sub> (SO<sub>2</sub>) and NO<sub>x</sub> (NO-NO<sub>2</sub>) on activated carbon prepared from waste palm shells [7]. Sumathi et al. (2010) introduced the impregnated carbon-based sorbents for the simultaneous removal of SO<sub>2</sub> and NO<sub>x</sub> from simulated

---

\*Corresponding author: jmjung@jbnu.ac.kr

†These authors were equally contributed to this article.

flue gas [8]. Goncalves et al. (2011) studied the effect of surface chemistry (nature and amount of oxygen groups) on the removal of ammonia using a modified resin-based activated carbon [9]. Li et al. (2011) conducted surface modification of coconut-shell-based activated carbon for the improvement of hydrophobic volatile organic compound (VOC) removal [10]. Wei et al. (2012) employed granular bamboo-derived activated carbon for high CO<sub>2</sub> adsorption [11]. Yang et al. (2015) synthesized a highly cost-effective nitrogen-doped porous coconut-shell-based CO<sub>2</sub> sorbent by combining ammoxidation with KOH activation [12]. Travlou et al. (2016) introduced nitrogen-doped activated-carbon-based ammonia sensors [13]. Khaleed et al. (2017) investigated the effect of activated carbon on the enhancement of the CO-sensing performance of NiO [14].

It is difficult, however, to form and process activated carbon on its own into a conductor with a three-dimensional (3D) structure. This has limited the quantification of sensor performance and made it difficult for activated carbon to be used as a conductor for gas sensing.

Therefore, this study aims to develop a sensor module that can be applied to highly sensitive gas sensors by proposing a method to process a new 3D composite conductor based on activated carbon. Fig. 1 shows a schematic of an activated-carbon–PEDOT:PSS composite conductor mounted on a polydimethylsiloxane (PDMS)-based gold electrode. To improve the electrical conductivity of the activated-carbon–PEDOT:PSS composite conductor, the composite conductor was fabricated as a 3D structure using PEDOT:PSS as a conductive binder. In addition, ethylene glycol and silver nanoparticles were added to improve the sensitivity and response time. It is expected that activated-carbon–PEDOT:PSS composite conductors absorb ethanol molecules, causing a change in the resistance of the conductor, making gas detection possible. After installing the fabricated 3D activated-carbon–PEDOT:PSS composite conductor in a sensor module, the performance of the sensor was assessed by measuring the electrical conductivity change, response time, and recovery time according to the pressure of the ethanol gas.

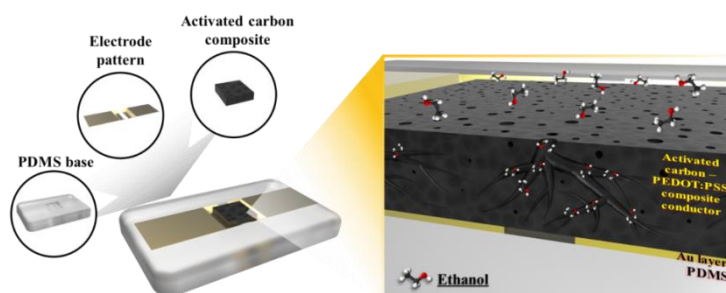


Fig. 1. Schematic of ethanol molecule adsorption mechanism of the activated-carbon–PEDOT:PSS composite conductor.

## 2. Experimental

### 2.1. Activated carbon and PEDOT:PSS

Among various activated carbons, four candidates—HP90N (Jacobi, Kalmar, Sweden), SPC-10 (Shinki Chemical, Gyeongnam, South Korea), SPW-10 (Shinki Chemical, Gyeongnam, South Korea), and JP-1 (Jeil Activated Carbon, Gyeonggi, South Korea)—were selected for use in an activated-carbon–PEDOT:PSS composite conductor based on the data provided by the manufacturers.

PEDOT:PSS (Clevios PH1000, Heraeus, Hanau, Germany) used in the activated-carbon–PEDOT:PSS composite conductor had a solid content of 1.0–1.3 wt% (in water), a PEDOT:PSS ratio of 1:2.5, an average particle size of 30 nm, and a specific resistance of up to 0.0012 Ω·cm.

## 2.2. Activated carbon pulverization

The activated carbons were pulverized using a ball mill (PM 100, Retsch GmbH, Haan, Germany) to increase the contact area between the activated carbon and the gas, and to improve the formability of the conductor. After placing the activated carbon and 14 stainless beads in the ball mill, pulverization was performed for a total of 60 min at 400 rpm. Pulverization was performed for 30 min, with the rotational direction changing every 5 min. After a 5-min break to allow the activated carbon and the inside of the ball mill to cool, pulverization was performed again for 30 min.

A crucible and an electric furnace capable of withstanding high temperatures were prepared to measure the ash content, which affects the adsorption performance of the activated carbon. For the ash analysis of the activated carbon, the crucible was placed inside the electric furnace at 650 °C, heated for 1 h, and cooled to room temperature in a desiccator in accordance with ASTM D2866. Next, 0.5 g of activated carbon was placed in the crucible, and the weight was measured to within 0.1 mg. After the crucible with the activated carbon was placed in the electric furnace, it was heated at 150 °C for 3 h to remove moisture, and heated again at 650 °C for 8 h. The crucible was then cooled to room temperature in a desiccator, and the weight was measured to determine the ash content. The ash content was calculated as the ratio of the ash remaining in the crucible after the experiment to the weight of the activated carbon placed at the beginning of the analysis.

## 2.3. BET specific surface area analysis

A specific-surface-area-measuring device (BELSORP-max, BEL JAPAN, Osaka, Japan) was used to measure the specific surface area of the activated carbon. The sample was preprocessed at 250 °C for 12 h before being loaded into the device to desorb the moisture or gases that were adsorbed by the activated carbon pores. The measurement was conducted using N<sub>2</sub> gas under a 77-K isothermal condition with varying pressure.

## 2.4. Assessment of silver nanoparticle dispersion in the conductor using EDS mapping

To identify the dispersion of silver nanoparticles in the conductor, mapping was performed using energy-dispersive X-ray spectroscopy (EDS) (EDAX, AMETEK, NJ, USA). Scanning was conducted 32 times, and the map data for the detected silver nanoparticles were overlaid with the SEM image of the conductor.

## 2.5. E-beam deposition for electrode fabrication

Gold was deposited on the gas sensor module base using an e-beam evaporator (KVE-C25096, Korea Vacuum Tech, Gyeonggi, South Korea). First, patterning was performed on the base using polyimide tape. To enhance the adhesion between the base and the gold deposition layer, 20 nm of titanium was deposited, and then 200 nm of gold was deposited; the deposition speed was 1 Å/s.

## 2.6. Fabrication of the activated-carbon–PEDOT:PSS composite conductor

A mold for the composite conductor was manufactured to fabricate the 3D activated-carbon–PEDOT:PSS composite conductor. The mold used after PDMS was cured to a 1-mm thickness, and a square hole of 8 mm × 8 mm was prepared. The mold was manufactured by attaching the PDMS and slide glass after performing plasma processing.

To fabricate the 3D activated-carbon–PEDOT:PSS composite conductor, 5 wt% silver nanoparticles (500 nm, SP-006SM, Incheon, South Korea) were inserted into the PEDOT:PSS solution and dispersed at 40 kHz for 1 h using a sonicator (BRANSON 3800 sonicator, BRANSON, CT, USA). The moisture in the solution was evaporated while being stirred on a 75 °C hot plate for 45 min to increase the viscosity of the solution. The activated carbon and ethylene glycol corresponding to 5 wt% of the initial PEDOT:PSS solution were added to the PEDOT:PSS solution with dispersed silver nanoparticles and stirred for 30 min using a vortex mixer (Vortex-Genie2, Scientific Industries, NY, USA). The obtained mixed solution was added in

350- $\mu$ L quantities into each mold for the composite conductor and dried under three different temperature conditions (4  $^{\circ}$ C, 25  $^{\circ}$ C, and 75  $^{\circ}$ C). When the resistance of the conductor with silver nanoparticles was compared with that of the conductor without, the average resistance of the conductor with 5 wt% silver nanoparticles was  $24 \pm 4 \Omega$ , whereas that of the conductor without was seven times higher, at  $141 \pm 17 \Omega$ .

## 2.7. Fabrication and assembly of a base for a gas sensor module

To fabricate a gas sensor module base, a mold for the base was manufactured first. The mold was fabricated using a 3D printer (X-Fab, DWS, Vicenza, Italy) of the stereolithography apparatus (SLA) type. PDMS mixed with a curing agent at a 10:1 ratio was used to fill the fabricated mold and cured in an oven at 75  $^{\circ}$ C for 8 h. Fig. 2 shows the configuration of the gas sensor module. The gas sensor module base with gold-deposited electrodes and the activated-carbon–PEDOT:PSS composite conductor were assembled using silver epoxy as an adhesive and cured at 65  $^{\circ}$ C for 1 h.

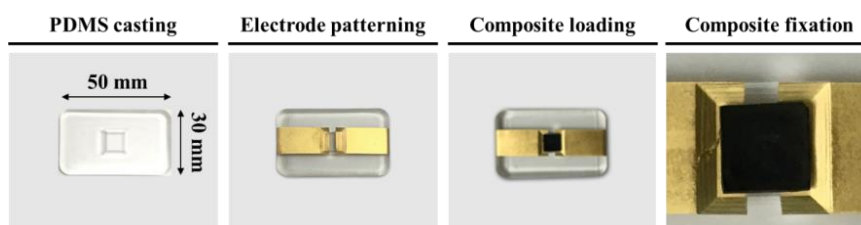


Fig. 2. Fabrication process for an activated-carbon–PEDOT:PSS composite conductor gas sensor module.

## 2.8. Experimental setup of gas adsorption system

Fig. 3 shows the experimental setup for gas adsorption. The experiment was conducted with a source level of 5 V, a temperature of 20  $^{\circ}$ C, and an initial pressure of 10 mTorr.  $N_2$  was used as the carrier gas, and the changes in the resistance of the activated-carbon–PEDOT:PSS gas sensor module were observed while the pressure of the ethanol gas was adjusted. The sensitivity, response time, and recovery time of the gas sensor module were measured according to the gas pressure. The sensitivity (%) was calculated as  $S = \frac{\Delta R}{R_0} \times 100 \%$ , where  $R_0$  is the initial resistance value and  $\Delta R$  is the resistance variation after gas injection.

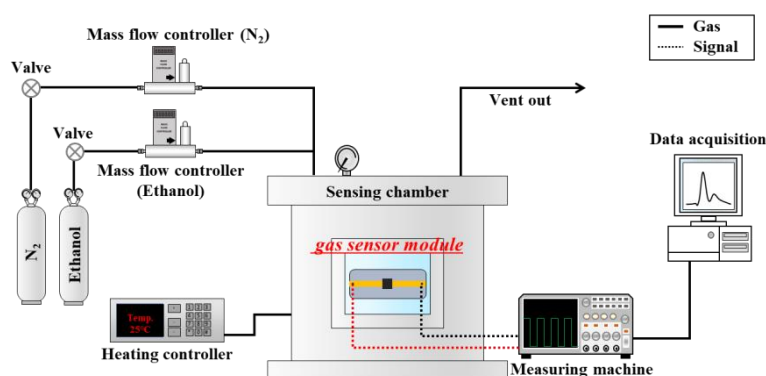


Fig. 3. Schematic of the experimental setup of the gas adsorption system for the activated-carbon–PEDOT:PSS composite gas sensor module.

### 3. Results and discussion

BET analysis and ash content analysis were conducted to assess the performance of the activated carbon pulverized for 60 min. The results are shown in Table 1. Among the four activated carbons, HP90N exhibited the largest specific surface area of  $1511 \text{ m}^2/\text{g}$ , meaning that it has the most micropores. HP90N also showed the highest pore volume,  $1.378 \text{ cm}^3/\text{g}$ , indicating that it may adsorb more gas. HP90N had the largest average pore size of 3.6 nm. This means that micropores, which perform adsorption, and pores, which become the movement paths of adsorbates, are developed appropriately. The ash content of HP90N was the lowest at 1.84%. The low content of ash, which interrupts pore development and interferes with gas adsorption by filling or blocking micropores, indicates that HP90N exhibits excellent performance in adsorbing gas. As HP90N exhibited the best adsorption performance when the specific surface area, pore volume, average pore size, and ash content were considered, it was used to fabricate the 3D activated-carbon–PEDOT:PSS composite conductor.

Table 1. Comparison of BET surface area analysis and ash content analysis of various activated carbons.

Activated carbon	$S_{\text{BET}}$ ( $\text{m}^2/\text{g}$ )	$V_{\text{total}}$ ( $\text{m}^3/\text{g}$ )	$d_{\text{mean}}$ (nm)	Ash Content (%)
HP90N	1511	1.378	3.6	1.84
SPW-10	938.3	0.527	2.2	19.6
SPC-10	1169	0.5636	1.9	3.2
JP-1	587	0.4228	2.9	21.0

Fig. 4 shows the SEM images of HP90N and its density distribution according to particle size. The initial average particle size of HP90N was  $22 \mu\text{m}$ . Because of pulverizing HP90N using a ball mill for 30 min, the average particle size decreased to  $7.5 \mu\text{m}$ . The average particle size of HP90N pulverized for 60 min was  $5.4 \mu\text{m}$ . The average particle size decreased as the pulverization time increased.

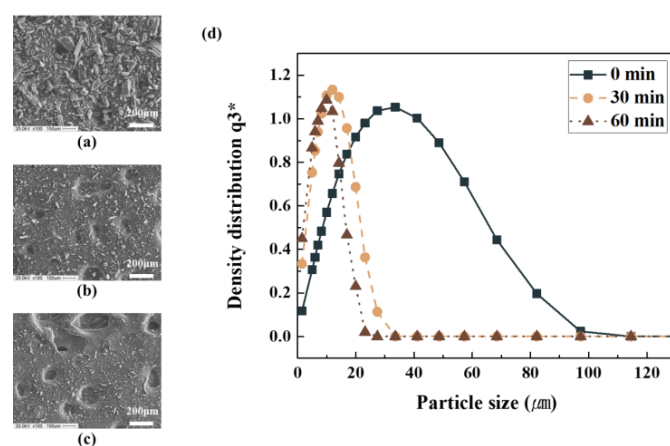


Fig. 4. Comparison of particle size of raw activated carbon and pulverized activated carbon. (a) Raw activated carbon, (b) activated carbon pulverized for 30 min, (c) activated carbon pulverized for 60 min, and (d) density distribution of particle size with pulverizing time.

Silver nanoparticles and ethylene glycol were added to the 3D activated-carbon–PEDOT:PSS composite conductor to improve the performance characteristics of the gas sensor module, such as sensitivity and response time. The electrical conductivity increased sharply when 5 wt% ethylene glycol was added. When 10 wt% was added, the shrinkage of the composite conductor volume increased, and 5 wt% silver nanoparticles were added. When more than 5 wt% silver nanoparticles were added, PEDOT:PSS reduced cohesion between the activated carbon and silver nanoparticles, resulting in breakage and cracks in the composite conductor during drying.

Fig. 5 shows the cracks in the activated-carbon–PEDOT:PSS composite conductor according to the drying conditions and an SEM image with dispersed silver nanoparticles. As shown in Fig. 5(a), cracks occurred in the activated-carbon–PEDOT:PSS composite conductor when it was dried at 75 °C, and distortion occurred when dried at 25 °C. When it was dried at 4 °C, however, no distortion or cracks occurred. Contraction occurs in composite conductors when they are dried, and residual stress occurs owing to the difference in drying speeds between the upper and lower parts. As the upper part dries faster than the lower part, compressive stress occurs in the upper part and tensile stress occurs in the lower part, resulting in distortion and cracks. At 4 °C, no distortion or cracks occurred because the drying speed of the upper part was similar to that of the lower part.

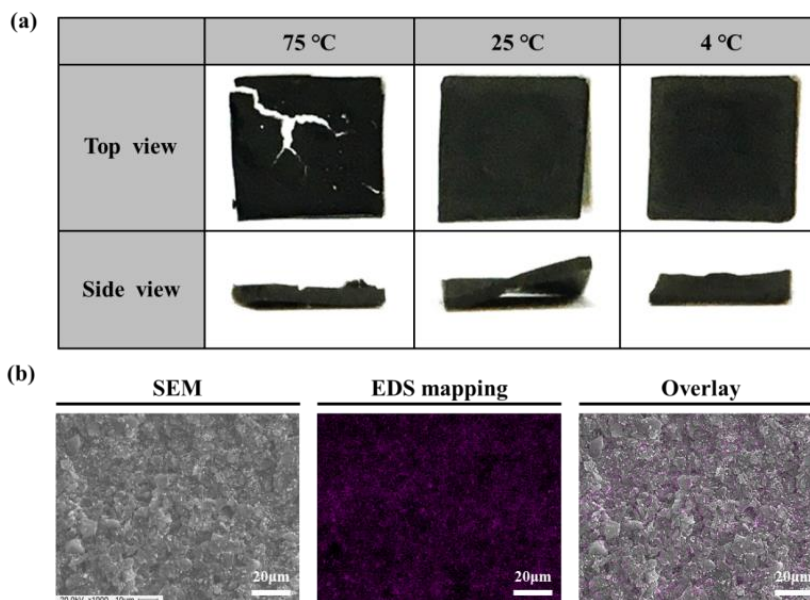


Fig. 5. Results of (a) the phenomenon of the activated-carbon composite with respect to the drying conditions, and (b) SEM image and EDS analysis of the activated carbon with silver nanoparticles.

As shown in the SEM image of the surface of the composite conductor in Fig. 5(b), the activated carbon was not covered with PEDOT:PSS, which was used as a binder. Therefore, it is expected that PEDOT:PSS will not affect the adsorption performance of the activated carbon. On overlaying the SEM image of the composite conductor with the silver-nanoparticle mapping image, it was confirmed that silver nanoparticles were dispersed well in the composite conductor.

Fig. 6(a) shows the repeatability assessment of the activated-carbon–PEDOT:PSS composite conductor at an ethanol gas pressure of 500 mTorr and an ambient temperature of 25 °C. When the valve for ethanol injection was opened, the ethanol gas was adsorbed on the activated-carbon–PEDOT:PSS composite conductor, thereby dramatically increasing the resistance. The average response time of the composite conductor was approximately 600 s, and the average recovery time was approximately 600 s. As a result of testing three conductors three times each, the sensitivity of the ethanol gas was found to be approximately  $0.15\% \pm 0.02$ .

Fig. 6(b) shows the resistance change according to the adsorption of the ethanol molecules as the pressure of the ethanol gas was varied between 250 and 1000 mTorr. The response time was

approximately 470 s, and the recovery time was approximately 412 s at 250 mTorr. They were approximately 610 and 306 s at 500 mTorr, and 609 and 266 seconds at 1000 mTorr, respectively. The recovery time tended to be shorter as the pressure of the ethanol gas increased, indicating that the desorption of ethanol molecules in the pores of the composite conductor accelerated as the partial pressure difference of the ethanol gas in the chamber increased. As a result of testing three conductors three times each, the sensitivity of the composite conductor to ethanol was  $0.04\% \pm 0.01$  at 250 mTorr,  $0.14\% \pm 0.02$  at 500 mTorr, and  $0.19\% \pm 0.025$  at 1000 mTorr, on average. Depending on the pressure increase of the ethanol gas, the sensitivity of the composite conductor increased approximately 3.5 times at 500 mTorr, and 4.75 times at 1000 mTorr, compared to that at 250 mTorr. The composite conductor with silver nanoparticles can detect sensitive resistance changes, and its applicability as a gas sensor was confirmed.

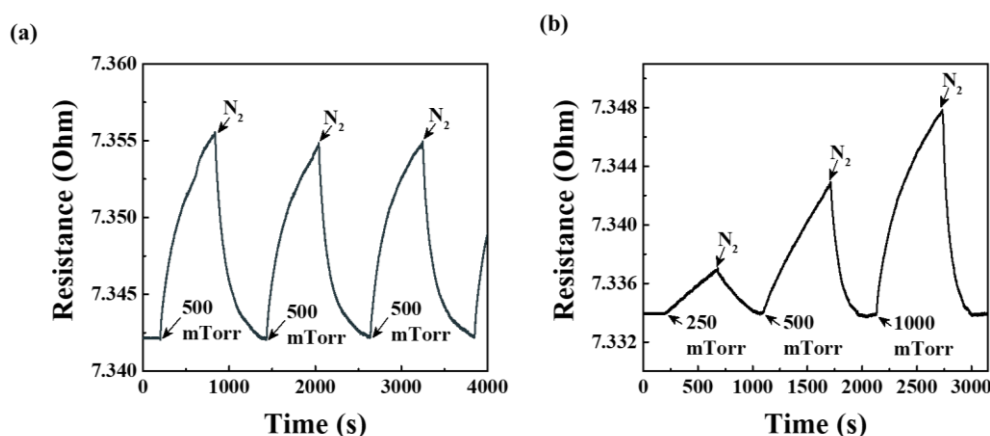


Fig. 6. Result of ethanol adsorption on the activated-carbon composite gas sensor module. (a) The evaluation of repeatability for ethanol at 500 mTorr, and (b) the change in resistance with ethanol concentration (250 mTorr, 500 mTorr, and 1000 mTorr).

#### 4. Conclusions

In this study, activated carbon was quantified by forming and processing it into a 3D structure, and a highly sensitive activated-carbon–PEDOT:PSS composite conductor for a gas sensor module was developed using the structure. The electrical conductivity of the activated-carbon–PEDOT:PSS composite conductor was improved by adding ethylene glycol and silver nanoparticles to accelerate oxidation and reduction reactions caused by gas adsorption.

To enhance the formability and processability of the activated-carbon–PEDOT:PSS composite conductor, it was freeze-dried at 4 °C, thereby preventing cracks and distortion caused by residual stress. On testing the adsorption of the composite conductor using ethanol gas, sensitive resistance changes caused by the ethanol molecules adsorbed on the activated carbon were confirmed. In this study, the applicability of activated carbon to gas sensors was confirmed, and it is expected that the results of this study will develop into a widely applicable technology in the field of biosensors in the future.

#### Acknowledgements

This research was supported by grants (20170328-A-002) from the Jeonbuk Research & Development Program, funded by Jeonbuk Province. This work was supported by a National Research Foundation of Korea (NRF) grant funded by the Korean government (MSIP) (NRF-2016R1C1B2014747 and NRF-2017R1A4A1015681).

## References

- [1] T. H. Wang, S. X. Tan, C. H. Liang. *Carbon* **47**, 1880 (2009).
- [2] L. Li, P. A. Quinlivan, D. R. U. Knappe. *Carbon* **40**, 2085 (2002).
- [3] D. Savova, E. Apak, E. Ekinci, F. Yardim, N. Petrov, T. Budinova, M. Razvigorova, V. Minkova. *Biomass Bioenerg* **21**, 133 (2001).
- [4] Y. C. Chiang, P. C. Chaing, C. P. Huang. *Carbon* **39**, 523 (2001).
- [5] I. Mochida, Y. Korai, M. Shirahama, S. Kawano, T. Hada, Y. Seo, M. Yoshikawa, A. Yasutake. *Carbon* **38**, 227 (2000).
- [6] K. J. Kim, C. S. Kang, Y. J. You, M. C. Chung, M. W. Woo, W. J. Jeong, N. C. Park, H. G. Ahn. *Catalysis Today* **111**, 223 (2006).
- [7] S. Sumathi, S. Bhatia, K. T. Lee, A. R. Mohamed. *Science in China Series E: Technological Sciences* **52**, 198 (2009).
- [8] S. Sumathi, S. Bhatia, K. T. Lee, A. R. Mohamed. *J Hazard Mater* **176**, 1093 (2010).
- [9] M. Goncalves, L. Sanchez-Garcia, E. Oliveira Jardim, J. Silvestre-Albero, F. Rodriguez-Reinoso. *Environ Sci Technol* **45**, 10605 (2011).
- [10] L. Li, S. Liu, J. Liu. *J Hazard Mater* **192**, 683 (2011).
- [11] H. Wei, S. Deng, B. Hu, Z. Chen, B. Wang, J. Huang, G. Yu. *ChemSusChem* **5**, 2354 (2012).
- [12] M. Yang, L. Guo, G. Hu, X. Hu, L. Xu, J. Chen, W. Dai, M. Fan. *Environ Sci Technol* **49**, 7063 (2015).
- [13] N. A. Travlou, C. Ushay, M. Seredych, E. Rodriguez-Castellon, T. J. Bandoz. *Acs Sensors* **1**, 591 (2016).
- [14] A. A. Khaleed, A. Bello, J. K. Dangbegnon, D. Y. Momodu, M. J. Madito, F. U. Ugbo, A. A. Akande, B. P. Dhonge, F. Barzegar, O. Olaniyan, B. W. Mwakikunga, N. Manyala. *Journal of Alloys and Compounds* **694**, 155 (2017).